A&A 383, 125–136 (2002)
DOI: 10.1051/0004-6361:20011741

Astronomy & Astrophysics

The M 81 group of galaxies: New distances, kinematics and structure⋆,⋆⋆

I. D. Karachentsev[1], A. E. Dolphin[2], D. Geisler[3], E. K. Grebel[4], P. Guhathakurta[5,⋆⋆⋆], P. W. Hodge[6], V. E. Karachentseva[7], A. Sarajedini[8], P. Seitzer[9], and M. E. Sharina[1,10]

[1] Special Astrophysical Observatory, Russian Academy of Sciences, N. Arkhyz, KChR, 369167, Russia
[2] Kitt Peak National Observatory, National Optical Astronomy Observatories, PO Box 26732, Tucson, AZ 85726, USA
[3] Departamento de Física, Grupo de Astronomía, Universidad de Concepción, Casilla 160-C, Concepción, Chile
[4] Max-Planck-Institut für Astronomie, Königstuhl 17, 69117 Heidelberg, Germany
[5] UCO/Lick Observatory, University of California at Santa Cruz, Santa Cruz, CA 95064, USA
[6] Department of Astronomy, University of Washington, Box 351580, Seattle, WA, USA
[7] Astronomical Observatory of Kiev University, 04053, Observatorna 3, Kiev, Ukraine
[8] Department of Astronomy, University of Florida, Gainesville, FL 32611, USA
[9] Department of Astronomy, University of Michigan, 830 Dennison Building, Ann Arbor, MI 48109, USA
[10] Isaac Newton Institute, Chile, SAO Branch

Received 25 September 2001 / Accepted 5 December 2001

Abstract. We present Hubble Space Telescope/WFPC2 images of the galaxies NGC 2366, NGC 2976, NGC 4236, IC 2574, DDO 53, DDO 82, DDO 165, Holmberg I, Holmberg II, Holmberg IX, K52, K73, BK3N, Garland, and A0952+69 in the M 81 complex. Their true distance moduli, derived from the brightness of the tip of the red giant branch, lie in the range of $27\overset{\mathrm{m}}{.}52$ (NGC 2366) to $28\overset{\mathrm{m}}{.}30$ (DDO 165), with a median of $27\overset{\mathrm{m}}{.}91$, which is typical for other known M 81 group members. Using distances and radial velocities of about 50 galaxies in and around the M 81/NGC 2403 complex, we find the radius of the zero-velocity surface of the M 81 group to be $R_0 = (1.05 \pm 0.07)$ Mpc, which yields a total mass $M(R_0) = (1.6 \pm 0.3) \times 10^{12}\ M_\odot$ and a total mass-to-luminosity ratio $M(R_0)/L_B = (38 \pm 7)\ M_\odot/L_\odot$. The total mass within R_0 agrees well with the sum of masses estimated via the virial theorem ($1.2 \times 10^{12}\ M_\odot$) and from orbital motions ($2.0 \times 10^{12}\ M_\odot$) of companions around M 81 and NGC 2403. We suggest that most of the dark matter in the group is concentrated around the luminous matter, allowing us to explain the observed asymmetry of the peculiar motions of the M 81 companions. M 81 itself has a peculiar velocity of about 130 km s^{-1} with respect to the local Hubble flow, but the centroid of the M 81/NGC 2403 complex is almost at rest with respect to Hubble flow ($v_{\rm pec} < 35$ km s^{-1}).

Key words. galaxies: dwarf – galaxies: distances and redshifts – galaxies: structure – galaxies: kinematics and dynamics

1. Introduction

The association of galaxies around M 81 is one of the nearest prominent groups in the vicinity of the Local Group. Both of the groups have a similar morphological population and binary structure. According to Tammann & Sandage (1968) and de Vaucouleurs (1978), the M 81 group is an extended filament with an angular size of ∼25° around the two bright galaxies NGC 2403 and NGC 4236. The space between the M 81 group and the Local Group is the nearest example of a cosmic mini-void. It has a diameter of ∼3 Mpc and is apparently free of any galaxy brighter than $-9^{\rm m}$ in absolute magnitude. Until 1998 accurate distance moduli derived via Cepheid were known only for the two brightest galaxies M 81 (Freedman et al. 1994) and NGC 2403 (Freedman & Madore 1988). The lack of distance estimates to other galaxies in the group makes the analysis of its structure and kinematics difficult. According to Karachentsev (1996) the physical radius of the M 81 group does not exceed 8°, and all companions to M 81, both dwarf spheroidal (dSph) galaxies and dwarf irregular (dIrr) galaxies, lie within this radius.

Send offprint requests to: I. D. Karachentsev,
e-mail: ikar@luna.sao.ru

⋆ Based on observations made with the NASA/ESA Hubble Space Telescope. The Space Telescope Science Institute is operated by the Association of Universities for Research in Astronomy, Inc. under NASA contract NAS 5–26555.

⋆⋆ Figures 2 to 5 are only available in electronic form at http://www.edpsciences.org

⋆⋆⋆ Alfred P. Sloan Research Fellow.

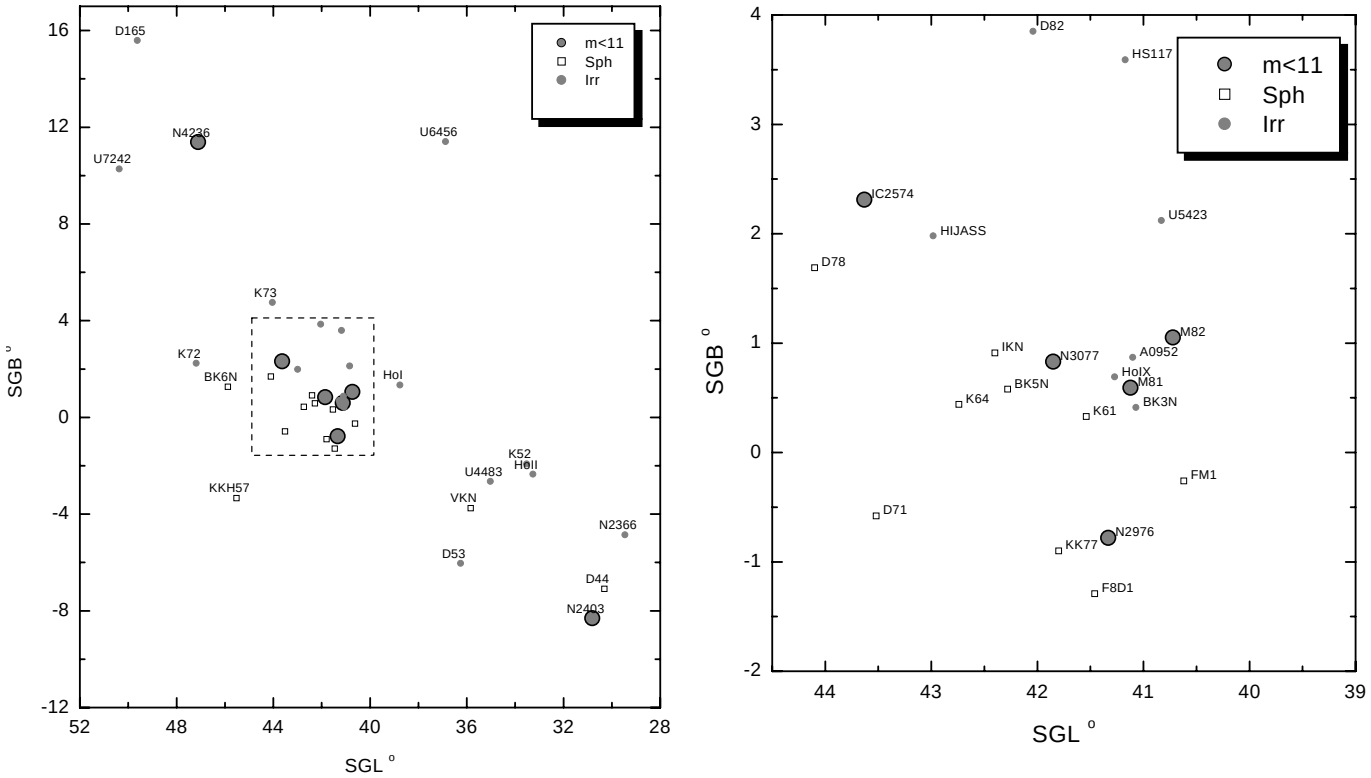

Fig. 1. The distribution of galaxies in the NGC 2403/M 81/NGC 4236 complex in supergalactic coordinates. Top: overview of the entire region, bottom: the central part of the M 81 group.

Since 1998 many more distance measurements in the M 81 group have become available thanks to observations with the Hubble Space Telescope (HST) and the use of the tip of the red giant branch (TRGB) method. Based on the brightness of the tip of the RGB, Caldwell et al. (1998), Lynds et al. (1998), and Sakai & Madore (1999) determined distances to four dwarf galaxies in the M 81 group: BK5N, F8D1, UGC 6456, and M 82. Many more probable members of the M 81 group were included in the snapshot survey of nearby galaxies (programs SNAP 8192 and 8601, PI: Seitzer) with the Wide Field and Planetary Camera 2 (WFPC2) aboard HST. As a result, we measured the TRGB distances to nine dSph galaxies (Karachentsev et al. 1999, 2000, 2001) and to one dIrr (Dolphin et al. 2001). In this paper we present new distance estimates for 13 late type galaxies observed with the HST. The new availability of accurate distances to most galaxies of the NGC 2403/M 81/NGC 4236 complex allows us to consider the 3D- structure, kinematics, and dynamics of the complex, a map of which is shown in Fig. 1. The stellar populations and star formation history of the observed galaxies will be discussed by us in the next paper.

2. HST WFPC2 photometry and color-magnitude diagrams

WFPC2 images of 15 objects in the M 81 group were obtained during 2000 July 11 to 2001 June 27 as part of our snapshot survey of probable nearby galaxies (SNAP 8601; Seitzer et al. 1999). Usually our target galaxies were centered on the WF3 chip, but for some bright targets the WFPC2 position was shifted towards the galaxy periphery to decrease a stellar crowding effect. The 600 s exposures were taken in F606W and F814W for each object. Digital sky survey (DSS) images (POSS-I,E) of the fifteen galaxies are shown in Fig. 2, on which the HST WFPC2 footprints are superimposed. The field size of the DSS images is $10'$ by $10'$ each.

The photometric reduction was made using the HSTphot stellar photometry package described in detail by Dolphin (2000a). After removing cosmic rays with the HSTphot *cleansep* routine, simultaneous photometry was performed on the $F606W$ and $F814W$ frames using *multiphot*, with aperture corrections for an aperture with $0\farcs5$ radius. Charge-transfer inefficiency corrections and calibrations were then applied based on the Dolphin (2000b) formulae, producing VI photometry for all stars detected in both images. Because of the relatively small field of the Planetary Camera (PC) chip, very few bright stars were available for the computation of an aperture correction. Thus the PC photometry was omitted from further analysis. Additionally, stars with a signal-to-noise ratio <5, $\mid \chi \mid > 2.0$, or $\mid$ sharpness $\mid > 0.4$ in each exposure were eliminated from the final photometry list. We estimate the uncertainty of the photometric zeropoint to be within $0\fm05$ (Dolphin 2000b).

Figure 3 shows mosaic images of the galaxies, where both filters were combined. The compass in each field indicates the North and East directions.

Table 1. Distance moduli for galaxies in the M 81 group.

Galaxy	RA (2000.0)	Dec	A_I	$I_{\rm TRGB}$	$(m-M)_0$
NGC 4236	12 16 43.2	+69 27 56	0.03	$24.22 \pm .22$	28.24
IC 2574	10 28 22.3	+68 24 58	0.07	$24.04 \pm .22$	28.02
NGC 2976	09 47 15.6	+67 54 49	0.14	$23.85 \pm .23$	27.76
Holm II	08 19 05.8	+70 42 50	0.06	$23.66 \pm .13$	27.65
NGC 2366	07 28 51.9	+69 12 18	0.07	$23.54 \pm .28$	27.52
DDO 165	13 06 26.7	+67 42 14	0.05	$24.30 \pm .19$	28.30
DDO 82	10 30 34.9	+70 37 09	0.08	$24.04 \pm .22$	28.01
Holm I	09 40 28.1	+71 11 10	0.09	$23.96 \pm .26$	27.92
Holm IX	09 57 32.0	+69 02 45	0.15	?	
DDO 53	08 34 06.5	+66 10 44	0.07	$23.78 \pm .15$	27.76
K 52	08 23 56.0	+71 01 45	0.04	$23.74 \pm .16$	27.75
Garland	10 03 42.7	+68 41 27	0.13	$23.99 \pm .24$	27.91
K 73	10 52 57.1	+69 32 58	0.04	$23.90 \pm .13$	27.91
BK3N	09 53 48.5	+68 57 51	0.16	$24.13 \pm .14$	28.02
A0952+69	09 57 32.6	+69 17 00	0.16	$24.05 \pm .12$	27.94

3. TRGB distances and integrated properties

In Fig. 4, I versus $(V-I)$ color magnitude diagrams (CMDs) for fifteen observed galaxies are presented. The total number of stars per image ranges from ∼20 000 (NGC 2976, NGC 4236) to ∼1000 (for the faintest objects). The left panels show the CMDs for the central WFC3 field. The middle panels represent the CMD for the neighbouring halves of WFC2 and WFC4 ($x <$ 425 pixels in WFC2 and $y < 425$ pixels in WFC4), and the right panels are comprised of stars found in the remaining outer halves of WFC2 and WFC4. Such a representation allows us to show the relative contribution of foreground stars when the galaxy diameter is comparable with the WF3 size.

As demonstrated by Lee et al. (1993), the TRGB is a reliable distance indicator that is relatively independent of age and metallicity. For metal-poor systems the TRGB may be assumed to be at $M_I = -4.05$ mag (Da Costa & Armandroff 1990). To determine the TRGB location we obtained the Gaussian-smoothed I-band luminosity function for red stars with colors $V-I$ within $\pm 0\overset{\rm m}{.}5$ with respect to the mean $< V-I >$ for expected RGB stars. Following Sakai et al. (1996), we used a Sobel edge-detection filter. The position of the TRGB was identified with the peak in the filter response function. The resulting luminosity functions and the Sobel filtered luminosity functions are shown in the upper and lower panels of Fig. 5, respectively. A summary of the resulting distance moduli for the observed galaxies is given in Table 1. Its columns contain: (1) galaxy name, (2) equatorial coordinates corresponding to the WF3 center, (3) Galactic extinction in the I-band from IRAS/DIRBE data (Schlegel et al. 1998), (4) position of the TRGB derived with the Sobel filter, (5) true distance modulus.

Some additional comments about the galaxy properties are given below. The galaxies are listed in a sequence of decreasing brightness.

NGC 4236. This galaxy of SBdm type has an angular dimension of $22' \times 7'$, much larger than the WFPC2 field of view. It is well resolved into stars (Sandage & Bedke 1988). Based on the brightest stars, de Vaucouleurs (1978) and Tikhonov et al. (1991) estimated its true distance modulus to be 27.65 mag and 27.56 mag, respectively. The CMD of NGC 4236 in Fig. 4 shows the presence of RGB and asymptotic giant branch (AGB) stars, as well as bright blue stars on the upper main sequence. We determined the TRGB position to be $I(\rm TRGB) = 24.22$ mag, which yields the true distance modulus $(m-M)_0 = 28.24$ mag. The error can be estimated as 1/2 of the peak width at 62% of its maximum and turns out to be $0\overset{\rm m}{.}22$. However, the mean-square scatter of TRGB positions derived separately for WF2, WF3, and WF4 is only $0\overset{\rm m}{.}04$.

IC 2574 = DDO 81. This galaxy of SABm type with angular dimensions of $13' \times 5'$ has distance modulus estimates of 27.72 mag (de Vaucouleurs 1978) and 27.89 mag (Tikhonov et al. 1991) via the brightest stars. In general its CDM in Fig. 4 looks similar to the NGC 4236 diagram. The derived TRGB position is $24\overset{\rm m}{.}04 \pm 0\overset{\rm m}{.}22$, but variations of TRGB positions between different chips do not exceed $0\overset{\rm m}{.}06$. From our data the true distance modulus is 28.02 mag.

Holmberg II = DDO 50 = UGC 4305. This irregular galaxy of the Magellanic (Im) type with numerous bright HII regions and blue stellar complexes has a size of $8' \times 6'$. From the brightest stars de Vaucouleurs (1978) and Tikhonov et al. (1992) estimated its distance modulus to be 27.79 mag and 27.78 mag, respectively. Our photometry gives $I(\rm TRGB) = 23.66 \pm 0.13$ mag, and $(m-M)_0 = 27.65$ mag.

NGC 2976. Unlike the two previous galaxies, NGC 2976 has a high surface brightness and is classified as Sc peculiar. Its central body of $6' \times 3'$ is spotted due to a lot of dust clouds and stellar complexes. Based on the luminosity of the brightest stars Karachentsev et al. (1991) estimated its distance modulus to be 28.30 mag. From our data the TRGB position for NGC 2976 corresponds to 23.85 ± 0.23 mag, which (with an $A_I = 0.14$ mag) yields a true distance modulus 27.76 mag.

NGC 2366 = DDO 42. This is an irregular galaxy with an angular size of $8' \times 3'$ and with a prominent star formation region on the southern edge (see Sandage & Bedke 1988), which is partially covered by the WF4. Photometry of the brightest stars in the galaxy yielded distance moduli 27.14 mag (de Vaucouleurs 1978) and 27.69 mag (Tikhonov et al. 1991). In our data we find the TRGB position at 23.54 ± 0.28 mag, giving the true distance modulus 27.52 mag. Note that the scatter of the $I(\rm TRGB)$ magnitude between different chips is only $0\overset{\rm m}{.}14$.

DDO 165 = UGC 8201. This irregular galaxy with an angular size of $3\overset{'}{.}5 \times 1\overset{'}{.}9$ has a very sharp southern boundary. DDO 165 was resolved into stars by Karachentsev et al. (1991), who derived a distance

modulus of 28.44 mag. In the HST photometry the TRGB is located at $24\overset{\mathrm{m}}{.}30 \pm 0\overset{\mathrm{m}}{.}19$, which corresponds to a true distance modulus of 28.30 mag.

DDO 82 = UGC 5692. This is a compact irregular galaxy with a size of $3'.2 \times 1'.8$. A bright red star is projected onto its southeastern side. In the central part of DDO 82 some dusty patches were noted (Karachentseva et al. 1985), which are seen also in the WF3 field (Fig. 3). From the brightest stars Karachentsev et al. (1994) determined $(m-M)_0 = 28.26$ mag. The HST photometry gives $I(\mathrm{TRGB}) = 24.04 \pm 0.22$ mag and a corresponding distance modulus of 28.01 mag. The area where DDO 82 is located has been observed repeatedly in the 21-cm line, but DDO 82 was never detected due to confusion with Galactic H I. In its optical spectra strong Hα emission with $V_{\mathrm{hel}} = +40$ km s^{-1} is seen (Karachentsev & Karachentseva 1984).

Holmberg I = DDO 63 = UGC 5139. This is an irregular dwarf galaxy of low surface brightness with an angular size of $3'.6 \times 3'.0$. Its distance modulus estimates via the brightest stars are discrepant: 27.68 mag (de Vaucouleurs 1978) and 29.11 mag (Tikhonov et al. 1992). The HST photometry yields $I(\mathrm{TRGB}) = 23.96 \pm 0.26$ mag and $(m-M)_0 = 27.92$ mag.

Holmberg IX = DDO 66 = K62 = UGC 5336. This dIrr galaxy has a size of $3'.5 \times 2'.8$ and an overall shape reminiscent of Holmberg I. It is situated several arcminutes away from the eastern spiral arm of M 81. On the H I map of Boyce et al. (2001) its location corresponds to a local density maximum with a heliocentric velocity of +50 km s^{-1}. Its distance modulus estimates from photometry of the brightest stars are rather discrepant: 28.8 mag (Sandage 1984), 30.1 mag (Hopp & Schulte-Ladbeck 1987), 27.5 mag (Davidge & Jones 1989), and 27.67 mag (Georgiev et al. 1991). Surface photometry of Holmberg IX carried out by Makarova (1999) yields an integrated magnitude of $B_{\mathrm{T}} = 14.53$ mag and an unusually blue integrated color, $(B-V)_{\mathrm{T}} = 0.22$ mag. Our attempt to determine the distance to Holmberg IX from the WFPC2 photometry meets with an unexpected problem. The CMD of the galaxy shows a well-populated red supergiant branch, but without clear signs of the RGB. Boyce et al. (2001) suggest Holmberg IX might be a young galaxy, condensing out of the H I tidal material. The apparent absence of an old stellar population looks like direct evidence for the recent formation of Holmberg IX. Obviously, this peculiar system requires further investigation with HST.

DDO 53 = UGC 4459 = VII Zw 238. The blue dwarf galaxy of $1'.5 \times 1'.3$ size was resolved into stars by Fisher & Tully (1979). Its distance modulus from the brightest stars is 27.44 mag (Karachentsev et al. 1994). Our HST photometry gives for DDO 53 $I(\mathrm{TRGB}) = 23.78 \pm 0.15$ mag, yielding a true distance modulus of 27.76 mag.

K 52 = M 81dwA. This low surface brightness dwarf galaxy with an angular size of $1'.3 \times 0'.7$ was found by Karachentseva (1968), and re-discovered by Lo & Sargent (1979), who detected it in the H I line. Tikhonov & Karachentsev (1993) estimated for K52 a distance modulus of 27.35 mag from the brightest blue stars. Our photometry gives $I(\mathrm{TRGB}) = 23.74 \pm 0.16$ mag, and $(m-M)_0 = 27.75$ mag.

Garland. The peculiar scattered structure with a size of $\sim 7' \times 4'$, consisting of blue stars and H II regions, was found on the southern side of NGC 3077 by Karachentseva et al. (1985) and nicknamed "Garland". Its small part was noted before by Barbieri et al. (1974) as a probable stellar complex belonging to NGC 3077. Spectral observations by Karachentsev et al. (1985) showed that the Garland has appreciable internal motions (± 35 km s^{-1}). Its mean radial velocity, $V_{\mathrm{h}} = +31$ km s^{-1}, is close to the radial velocity of NGC 3077, $V_{\mathrm{h}} = +14 \pm 4$ km s^{-1}. Sharina (1991) carried out photometry of the brightest stars in the Garland and derived a distance modulus of 27.76 mag. A concentration of neutral hydrogen in the Garland position was seen on the H I map of the M 81 group obtained by Appleton et al. (1981). Recently Heithausen & Walter (2000) revealed a giant molecular cloud in the same region with a mass of about $3 \times 10^7\, M_\odot$. The origin of the Garland remains unclear: either it is a young stellar complex in the NGC 3077 periphery, a tidal tail, or a separate dwarf galaxy disturbed by tidal interaction with NGC 3077.

Our HST photometry gives for the Garland field $I(\mathrm{TRGB}) = 23.99 \pm 0.24$ mag and $(m-M)_0 = 27.91$ mag. Unlike the blue stars, the distribution of RGB stars across the WFPC2 field shows them to be concentrated strongly towards the NGC 3077. Consequently, our estimate of the distance modulus applies in fact to NGC 3077, but not to the Garland. Recently the Garland region has been observed with WFPC2 by Sakai & Madore (2001). The location of their "Field II" overlaps partially with ours. They find the TRGB position to be at $24\overset{\mathrm{m}}{.}0 \pm 0\overset{\mathrm{m}}{.}1$ mag in excellent agreement with our estimate.

K 73. This is a small ($0'.6 \times 0'.4$) irregular dwarf galaxy well resolved into stars (Karachentseva et al. 1985). Its H I spectrum contains two emission lines with heliocentric velocities -132 km s^{-1} (Huchtmeier & Skillman 1998) and +115 km s^{-1} (van Driel et al. 1998). The recent H I observations by Huchtmeier (private communication) give a preference to the value of +115 km s^{-1} as belonging to the K73 itself rather than to the Local H I. Based on the luminosity of three the brightest blue stars Tikhonov & Karachentsev (1993) estimated the distance modulus of K73 to be 28.03 ± 0.4 mag. Our HST photometry yields a TRGB position corresponding to the distance modulus 27.91 ± 0.13 mag in good agreement with the previous estimate.

BK3N. This very faint dwarf system with an angular extent of $0'.4 \times 0'.3$ is situated $11'$ to the southwest from the M 81 center. The galaxy was discovered by Börngen & Karachentseva (1982) on the Tautenburg Schmidt telescope plates. Tikhonov & Karachentsev (1993) resolved BK3N into stars and derived a distance modulus of 27.23 mag via the three brightest blue stars. With $B_{\mathrm{T}} = 18.75$ mag (Makarova 1999), BK3N is the galaxy with

the faintest absolute magnitude known outside the Local Group. Our HST photometry (Fig. 4) shows that all the detected blue stars are concentrated within BK3N. In addition, a population of faint red stars is seen in the WF2, WF3, and WF4 fields. Assuming that they are RGB stars, we obtain $I(\mathrm{TRGB}) = 24.13 \pm 0.14$ mag, which yields a distance modulus of 28.02 mag. Because the red stars do not show any increase in density toward the main body of BK3N, we suggest that they may not actually be associated with BK3N, but could instead be part of the extended halo RGB population of M 81. The TRGB distance modulus agrees within errors with the distance modulus 27.80 ± 0.08 derived for M 81 from Cepheids (Freedman et al. 1994; Ferrarese et al. 2000). Hence BKN3 is very likely more distant than M 81 and observed through M 81's halo.

A0952+69 = Arp's loop. This ring-like structure of extremely low surface brightness was found by Arp (1965) around the northern side of M 81. The brightest part of this structure, A0952+69, situated 17′ NE from the M 81 center, is also seen as overdensity on the H I maps derived by Gottesman & Veliachev (1975) and Yun et al. (1994). On large-scale photographs of this part of Arp's loop Efremov et al. (1986) found a lot of very faint blue stars and diffuse objects, prompting them to suggest that there is ongoing star formation in the loop, probably stimulated by the interaction of M 81 with M 82 and NGC 3077.

The CMD derived with WFPC2 shows the presence of blue stars over the whole field of view. The brightest of them are $V \sim 22\overset{\mathrm{m}}{.}5$. Apart of them we recognize also red stars, which may belong to Arp's loop itself or to the periphery of the M 81 disk. The TRGB position for stars in the WF3 is $I(\mathrm{TRGB}) = 24.05 \pm 0.12$ mag, yielding a distance modulus 27.94 mag, which differs very little from the M 81 distance.

4. Structure and kinematics of the M 81 complex

The availability of accurate distance estimates and radial velocities for most the galaxies around M 81, NGC 2403, and NGC 4236 allows us to study the 3-D structure and kinematics of the nearest galaxy complex. Basic data on galaxies in the region are presented in Table 2. Its columns contain: (1) galaxy name, (2, 3) supergalactic coordinates, (4) angular separation Θ from M 81 in degrees, (5) radial velocity in km s^{-1} in the LG rest frame, (6) morphological type, (7) apparent integrated magnitude from NED or from Makarova (1999) and other recent sources, (8) Galactic extinction from Schlegel et al. (1998), (9) distance modulus, (10) linear distance to the galaxy in Mpc, where values with one decimal number correspond to rough distance estimates derived via the brightest stars (Karachentsev & Tikhonov 1994); when an individual distance estimate to a galaxy was absent (for instance, for Holmberg IX or IKN) the average group distance is adopted, (11, 12) projected (R_p) and de-projected spatial (R) separation of a galaxy from M 81, calculated as

$$R_\mathrm{p} = D_{\mathrm{M\ 81}} \cdot \sin\Theta, \quad \text{and}$$
$$R^2 = D^2 + D^2_{\mathrm{M\ 81}} - 2D \cdot D_{\mathrm{M\ 81}} \cdot \cos\Theta.$$

To avoid the loss of possible peripheric members of the complex, we included in Table 2 data on all known galaxies around M 81 with projected angular separations $\Theta < 30°$, and radial velocities $V_\mathrm{LG} < 500$ km s^{-1}. The distance moduli for some of these (NGC 3738, KKH34, UGC 6541, UGC 7298, NGC 5204, CamA, NGC 1560, CamB, NGC 3741, UGC A105, UGC 8508, and KK109) have been measured using data from our snapshot survey (Seitzer et al. 2002; Dolphin et al. 2002; Grebel et al. 2002). The objects in Table 2 are listed with increasing separation Θ from M 81. Apart from galaxies with known radial velocities and/or distance estimates, we included into the Table two dSph galaxies of extremely low surface brightness, IKN and VKN, discovered recently by I. D. Karachentsev and V. E. Karachentseva, as well as the object HIJASS J1021+6842 (H I cloud?) found by Boyce et al. (2001) in a blind H I survey of the M 81 group. For the two dSph galaxies DDO 78 and K61 we use the radial velocities measured by Sharina et al. (2002).

In Fig. 6 we present the resulting 3-D map of the M 81 group and its surroundings in the volume of $3.0 \times 1.7 \times 1.0$ Mpc in the supergalactic Cartesian coordinates. The three brightest spiral galaxies: NGC 2403, M 81, and NGC 4236 are shown as ellipsoids, and dIrr and dSph systems are shown as small filled and light circles, respectively. The observed 3-D distribution proves the suggestion of Tammann & Sandage (1968) regarding filamentary structure of the galaxy complex around M 81. However, the observed variation of the mean radial velocity from the nearby end of the filament (NGC 2403) to the far end (NGC 4236) does not fit the case of free expansion of that structure: NGC 4236 and its neighbours move away from the compact subgroup of M 81 companions, and NGC 2403 with its neighbouring dwarf galaxies approach the M 81. The distribution of dwarf spheroidal galaxies demonstrates much stronger concentration towards M 81 than the distribution of dIrrs. Such a morphological segregation is well known in the Local Group, as well as in many clusters of galaxies.

According to Sandage (1986) and Lynden-Bell et al. (1988) any sufficiently dense group or cluster may be characterized by a spherical "zero-velocity surface", which separates the group as overdensity against the homogeneous cosmic expansion. In case of spherical symmetry, the radius of the sphere, R_0, is related to the total mass of the group, M_0, and to the Hubble constant, H_0, as

$$M_0 = (\pi^2/8G) \cdot H_0^2 \cdot R_0^3, \qquad (1)$$

where G is the gravitation constant. For the Local Group the observed value of R_0 is 0.96 ± 0.05 Mpc (Karachentsev & Makarov 2001). The data of Table 2 allow us to estimate the radius of the zero-velocity surface for the M 81 group. As shown in Fig. 7, a galaxy with distance D from the LG,

Table 2. Galaxies in and around the NGC 2403/M 81/NGC 4236 complex.

Name	SGL	SGB	Θ	$V_{\rm LG}$ km s^{-1}	Type	$B_{\rm t}$	A_B	$(m-M)_0$	D Mpc	Rp kpc	R kpc	$(V-V_{\rm M\ 81})_{\rm p}$ km s^{-1}
M 81	41.°12	0.°59	0.°00	106	Sb	7.$^{\rm m}$69	0.$^{\rm m}$36	27.$^{\rm m}$80	3.63	0	0	0
HoIX	41.27	0.69	0.18	189	Ir	14.53	0.35		3.7:	11	11	82
BK3N	41.07	0.41	0.18	101	Ir	18.78	0.35	28.02	4.02	11	391	−5
A0952	41.10	0.87	0.28	143	Ir	16.8	0.37	27.94	3.87:	18	241	136
K61	41.54	0.33	0.52	23	sph?	15.25	0.30	27.78	3.60	33	44	57
M 82	40.72	1.05	0.62	360	Ir	9.06	0.58	27.74	3.53	39	107	−236
N3077	41.85	0.83	0.77	153	Ir	10.46	0.29	27.91	3.82	49	196	46
FM1	40.62	−0.26	0.98		sph	17.50	0.31	27.67	3.42	62	218	
BK5N	42.28	0.58	1.16		sph	17.4	0.25	27.89	3.78	73	168	
IKN	42.40	0.91	1.32		sph	17.0:	0.60		3.7:	84	110	
N2976	41.33	−0.78	1.38	139	Sm	10.94	0.30	27.76	3.56	87	111	−18
U5423	40.83	2.12	1.55	493	BCG	14.42	0.34		5.3	98	1674	386
K64	42.74	0.44	1.63		sph	15.46	0.25	27.84	3.70	103	126	
KK77	41.80	−0.90	1.64		sph	16.3	0.65	27.71	3.48	104	181	
F8D1	41.46	−1.29	1.91		sph	15.7	0.38	27.88	3.77	121	187	
HIJASS	42.98	1.98	2.32	187	HI		0.09		3.7:	147	164	40
HoI	38.76	1.34	2.47	285	Ir	13.64	0.21	27.92	3.84	156	265	147
DDO 71	43.52	−0.58	2.67	12	sph	15.95	0.37	27.72	3.50	169	211	59
HS117	41.17	3.59	3.00	116	Ir	16.5:	0.49		3.7:	190	204	9
IC2574	43.63	2.31	3.05	186	Sm	10.84	0.16	28.02	4.02	193	440	74
DDO 78	44.10	1.69	3.18	191	sph	15.8	0.12	27.85	3.72	201	223	42
DDO 82	42.04	3.85	3.38	191	Im	13.57	0.19	28.01	4.00	214	433	77
BK6N	45.88	1.27	4.81		sph	16.9	0.05	27.93	3.85	304	383	
K73	44.03	4.75	5.07	263	Ir	17.09	0.09	27.91	3.70	321	380	92
KKH57	45.52	−3.34	5.90		sph	17.86	0.09	27.97	3.93	373	491	
K72	47.18	2.23	6.28	466	Ir	15.00	0.05		7.4	397	3812	359
VKN	35.84	−3.75	6.83		sph	17.7:	0.34		3.4:	432	478	
U4483	35.02	−2.65	6.90	301	BCG	14.95	0.15	27.53	3.21	436	588	−122
K52	33.52	−1.93	8.00	267	Ir	16.35	0.09	27.75	3.55	505	507	0
DDO 53	36.25	−6.04	8.22	150	Ir	14.55	0.16	27.76	3.56	519	520	13
HoII	33.26	−2.36	8.40	312	Im	11.09	0.14	27.65	3.39	530	567	−59
U6456	36.87	11.40	11.60	97	BCD	14.28	0.16	28.23	4.43	730	1139	8
N4236	47.11	11.38	12.32	160	Sd	10.06	0.06	28.24	4.45	775	1190	57
N2366	29.46	−4.86	12.87	254	Im	11.68	0.16	27.52	3.19	809	881	−38
DDO44	30.31	−7.09	13.26		sph	15.64	0.19	27.52	3.19	833	901	
U7242	50.37	10.27	13.35	213	Ir	14.60	0.09		4.3	838	1137	92
N2403	30.80	−8.31	13.60	267	Sc	8.82	0.18	27.59	3.30	854	884	−18
KKH79	55.01	9.66	16.59	446	Ir	17.7	0.08		6.4	1036	3099	334
DDO 165	49.62	15.59	17.18	199	Im	12.85	0.10	28.30	4.57	1072	1538	92
N3738	59.56	1.79	18.47	310	Ir	12.13	0.05	28.40	4.75	1150	1741	180
KKH34	22.54	−0.41	18.61	298	Ir	17.1	1.08	28.57	5.18	1158	2090	183
N4605	55.47	12.02	19.67	278	Sm	10.89	0.06		5.2	1222	2160	167
N4068	62.95	4.93	22.26	290	Im	13.19	0.09		5.3	1375	2378	180
U6541	64.19	−0.79	23.12	303	Ir	14.23	0.09	27.99	3.96	1425	1555	122
U7298	63.89	6.63	23.50	253	Ir	15.95	0.10	28.10	4.17	1447	1674	125
N5204	59.40	17.85	24.91	341	Sm	11.73	0.05	28.24	4.45	1529	1918	184
CamA	16.09	1.87	25.06	157	Ir	14.85	0.93	27.89	3.78	1538	1614	62
N1560	16.03	0.79	25.09	169	Sd	12.16	0.81	27.63	3.36	1539	1541	48
N2537	41.42	−25.82	26.41	477	Sm	12.32	0.32		6.9	1615	3990	368
CamB	15.04	−4.21	26.50	264	Ir	16.71	0.94	27.60	3.31	1620	1621	54
N3741	67.96	−2.08	26.97	263	Ir	14.3	0.10	27.48	3.13	1646	1650	37
UA281	67.94	7.06	27.59	350	BCG	15.15	0.06		5.7	1681	2998	240
UA105	14.99	−9.26	27.82	280	Im	13.9	1.35	27.57	3.26	1694	1695	44
U8508	63.09	17.91	27.98	187	Ir	14.12	0.06	27.04	2.56	1703	1821	14
N4144	69.07	3.83	28.14	319	Scd	12.16	0.06		9.8:	1712	6817	231
KK109	70.24	−0.92	29.16	243	Ir	17.5	0.08	28.36	4.70	1769	2339	138
U4426	46.10	−28.52	29.50	399	Im	15.0	0.16		5.7	1787	3106	281
N1569	11.91	−4.92	29.69	105	BCG	11.86	3.02		2.5:	1798	1913	45
KKH87	60.42	23.98	29.95	475	Ir	16.1	0.05		6.8:	1812	4079	367

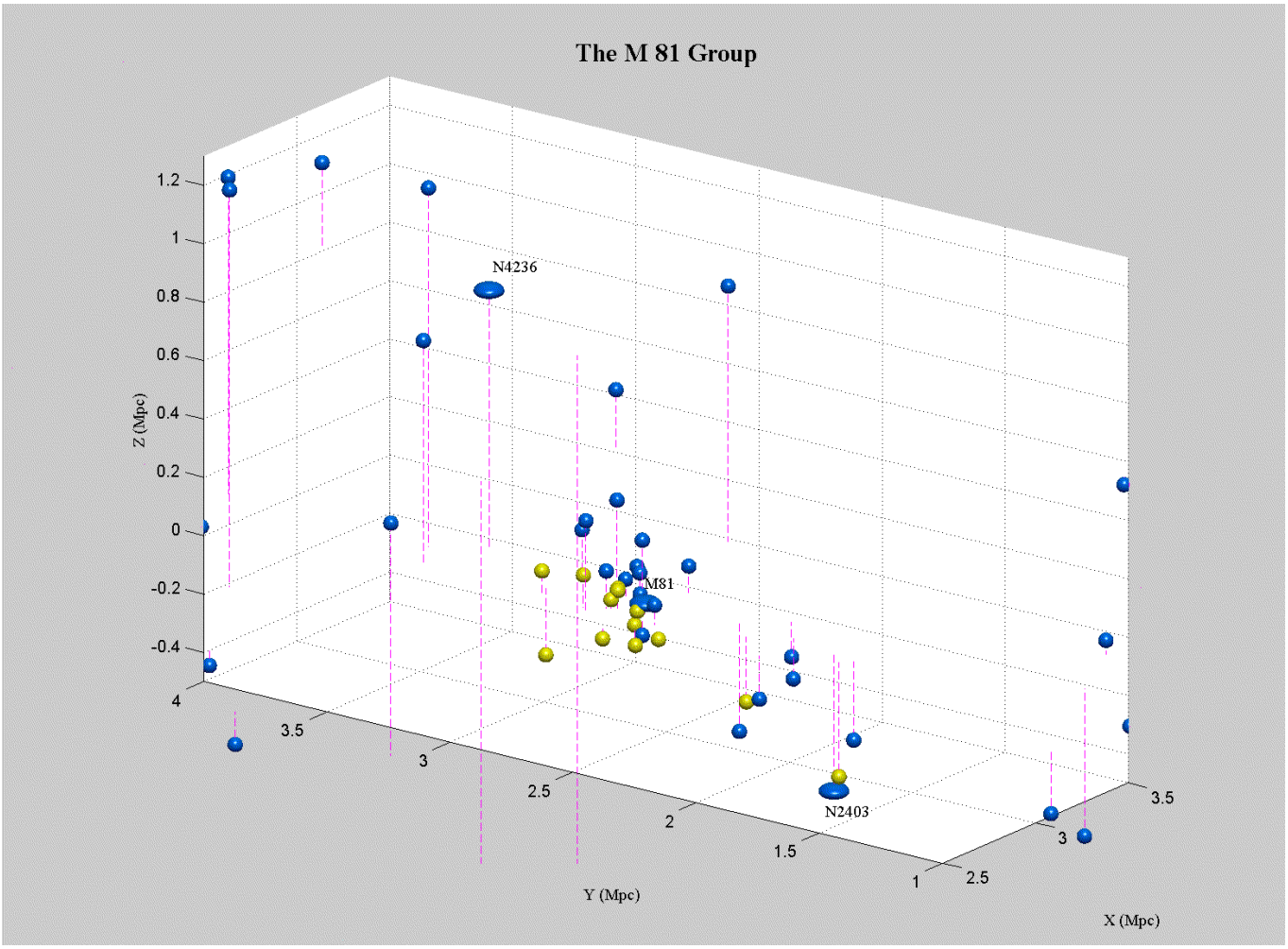

Fig. 6. The 3-dimensional view of the M 81 group and its surroundings in supergalactic Cartesian coordinates. The three brightest spirals NGC 2403, M 81, and NGC 4236 are show as ellipsoids, and dIrr and dSph galaxies are shown as small dark and light dots, respectively.

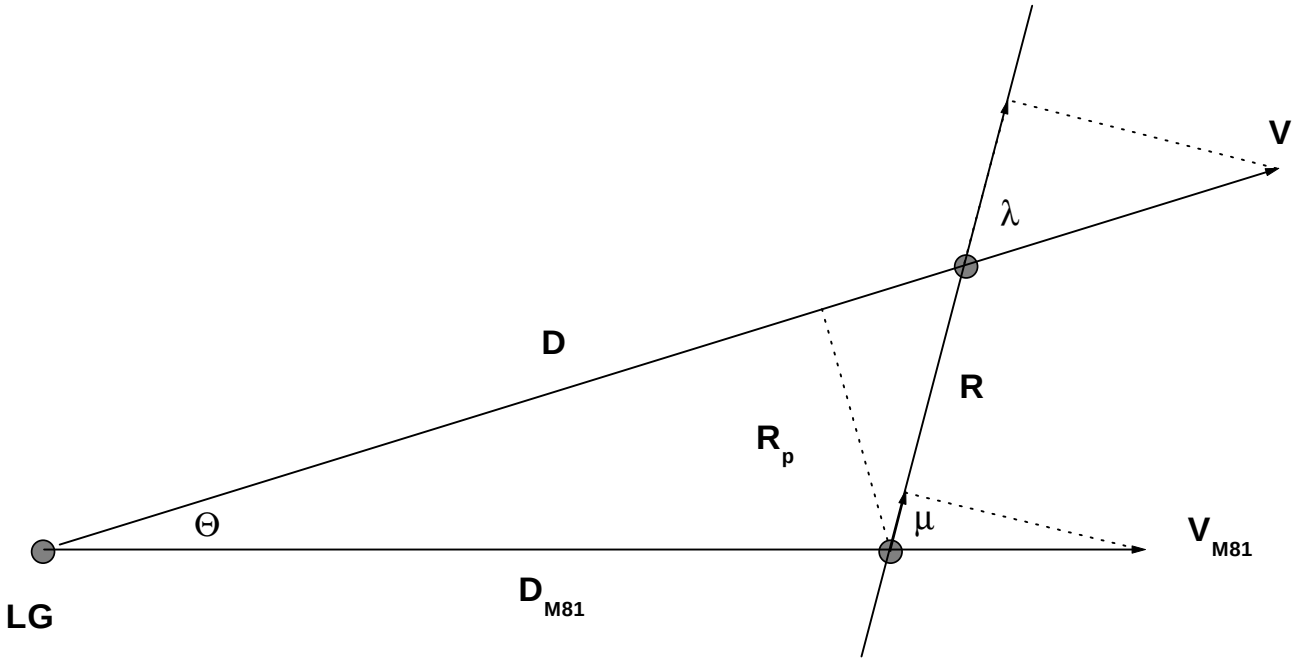

Fig. 7. A schematic disposition of a galaxy with respect to the M 81 and the Local Group.

radial velocity V, and angular separation Θ from M 81 has the following projected radial velocity with respect to M 81:

$$(V - V_{\rm M\ 81})_{\rm p} = V \cdot \cos\lambda - V_{\rm M\ 81} \cdot \cos\mu, \quad (2)$$

where $\mu = \theta + \lambda$, and $\mathrm{tg}\lambda = D_{\rm M\ 81} \cdot \sin\theta / (D - D_{\rm M\ 81} \cdot \cos\theta)$. Here we assumed that the peculiar velocities of the galaxies are small in comparison with velocities of the regular Hubble flow. The calculated values of $(V - V_{\rm M\ 81})_{\rm p}$ are presented in the last column of Table 2. As a result, Fig. 8 shows the $(V - V_{\rm M\ 81})_{\rm p} \propto R$ distribution for the galaxies in wide vicinity of M 81. The galaxies with accurate distances, derived from RGB stars or Cepheids, are indicated with filled squares, and the galaxies with rough distances (via the brightest stars) are marked with open squares. The distribution in Fig. 8 reveals several properties. 1) Among sufficiently distant galaxies with $R > 1$ Mpc there are no galaxies approaching M 81 (the region of cosmological expansion); 2) in the range of distances 0.55–1.0 Mpc we find only galaxies approaching M 81 (the infall zone); 3) within $R < 0.55$ Mpc there are galaxies both with negative as well as positive velocities with respect to M 81 ("virialized" zone). The data in Fig. 8 give us a radius for the zero-velocity surface of $R_0 = (1.05 \pm 0.07)$ Mpc, which is very close to the value of (0.96 ± 0.05) Mpc derived for the Local Group.

Note that the number of companions of M 81 with positive and with negative peculiar velocities is rather asymmetric, $\mathrm{N_+{:}N_-} = 13{:}3$. This asymmetry, already found by Arp (1982), may be caused by a selection effect when the H I line emission of galaxies with $V_{\rm h} < 0$ km s^{-1} is blended with strong Galactic emission. This explanation, however, requires a lot of missing galaxies in the M 81 group. Another possible explanation of the Arp paradox may lie in the considerable peculiar velocity of M 81 with respect to the group centroid ($\sim$50 km s^{-1}).

5. Mass estimates for the M 81 group

The galaxy M 81 with its morphological type Sb, absolute magnitude $M_B = -20.47$ mag, and amplitude of rotational velocity $V_{\rm m} \simeq 250$ km s^{-1} is very similar to the Milky Way and M 31. In the zone of its predominant gravitational influence, $R \sim 500$ kpc, 25 probable companions are known. We distinguished their names in Table 2 with bold print. At the moment, 16 of these objects have measured radial velocities, which allows us to estimate the group mass.

5.1. Virial mass estimate

The total mass of a group can be estimated from the virial balance of kinetic and potential energy of the system (Limber & Mathews 1960)

$$M_{\rm vir} = 3\pi N \cdot (N-1)^{-1} \cdot G^{-1} \cdot \sigma_{\rm v}^2 \cdot R_{\rm H}, \quad (3)$$

where N is the number of group members, $\sigma_{\rm v}^2$ is the dispersion of radial velocities with respect to the group centroid, and $R_{\rm H}$ is the mean projected harmonic radius of the group. For the 25 probable companions of M 81 we derive $R_{\rm H} = 57$ kpc, and for the 16 with known velocities we obtain $\sigma_{\rm v} = 84$ km s^{-1}. This yields the virial mass estimate

$$M_{\rm vir}(\mathrm{M\ 81}) = 0.94 \times 10^{12}\ M_\odot.$$

According to the criterion of group membership (Karachentsev 1996) relying on distances, velocities and luminosities of galaxies, the four irregular dwarf galaxies NGC 2366, Holmberg II, UGC 4483, and K52 may be considered companions of the Sc galaxy NGC 2403. We add to them also the dSph galaxy DDO 44, whose radial velocity is unknown. This subgroup has much lower dispersion of radial velocities, $\sigma_{\rm v} = 22$ km s^{-1}, but larger harmonic radius of $R_{\rm H} = 196$ kpc that leads to the virial mass

$$M_{\rm vir}(\mathrm{NGC\ 2403}) = 0.26 \times 10^{12}\ M_\odot.$$

5.2. Orbital mass estimate.

Bahcall & Tremaine (1981) and other authors noted that Eq. (3) is an inefficient mass estimator because the variance of the harmonic projected separations is logarithmically infinite. If a group contains a dominant massive galaxy, we may estimate its mass from the orbital motions of its companions, averaging the value $(R_{\rm p} \cdot \Delta V_{\rm r}^2)$. In the case of arbitrarily oriented Keplerian orbits with the eccentricity e we have the more robust mass estimator

$$M_{\rm orb} = (32/3\pi) \cdot G^{-1} \cdot (1 - 2e^2/3)^{-1} < R_{\rm p} \cdot \Delta V_{\rm r}^2 > \cdot \quad (4)$$

Using an average ellipticity of $e = 0.7$, we obtain for the 16 companions of M 81 a mass of

$$M_{\rm orb}(\mathrm{M\ 81}) = 1.63 \times 10^{12} M_\odot.$$

Note that the two companions K73 and Holmberg I with their large projected separations and high peculiar velocities give an essential input into the orbital mass estimate. Omitting these two objects drops the mass estimate to $0.8 \times 10^{12}\ M_\odot$. A similar uncertainty also takes place in the Local Group where including or excluding the dwarf galaxy Leo I can have a strong effect on the derived mass of the Milky Way. For the NGC 2403 subgroup this mass estimator yields

$$M_{\rm orb}(\mathrm{NGC\ 2403}) = 0.38 \times 10^{12}\ M_\odot.$$

It should be noted, however, that the "crossing time" of the NGC 2403 subgroup is $\sim$10 Gyr, hence, the subgroup has not yet reached the virialized state.

5.3. Total mass-to-luminosity ratio

From Eq. (1) with $R_0 = 1.05 \pm 0.07$ Mpc and $H_0 = 70$ km s^{-1} Mpc^{-1} the total mass M_0 of the M 81 group within the sphere of the zero-velocity surface is

$$M_0 = (1.6 \pm 0.3) \times 10^{12}\ M_\odot,$$

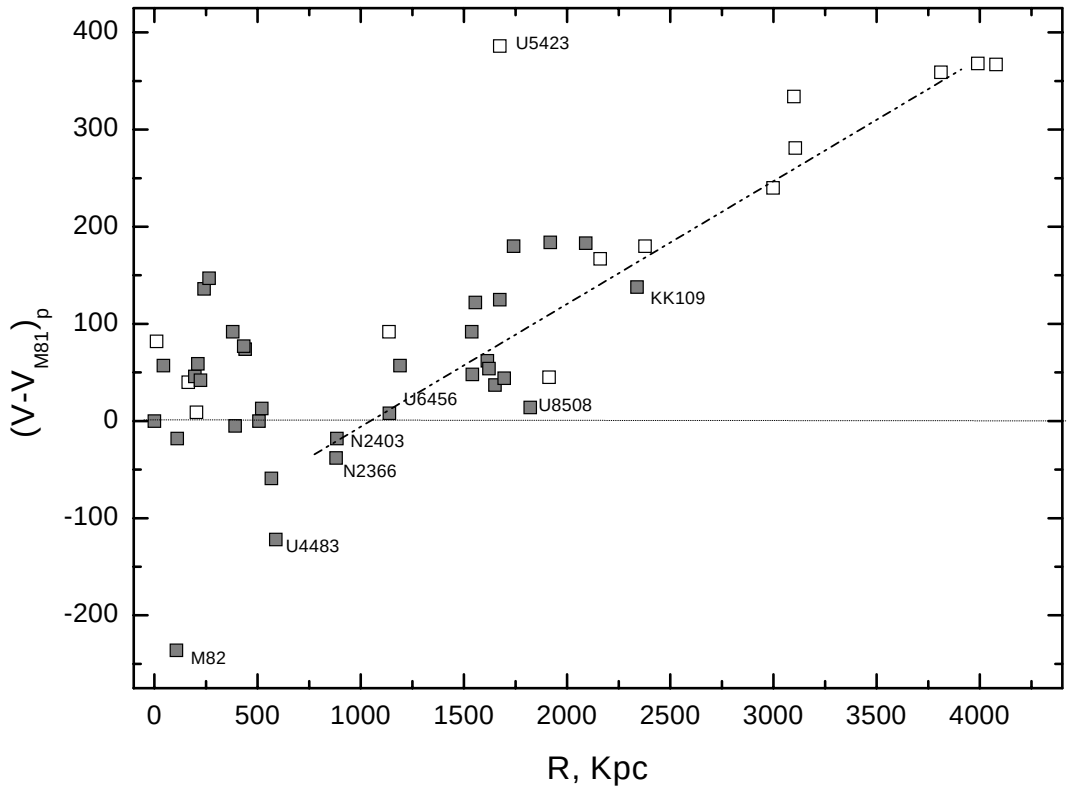

Fig. 8. Distribution of the radial velocity difference and the spatial distance of nearby galaxies with respect to M 81. Galaxies with accurate and with rough distance estimates are indicated by filled and open squares, respectively. These data yield a radius of the zero-velocity surface of (1.05 ± 0.07) Mpc.

where the error of the mass estimate corresponds formally to the error of ± 0.07 Mpc for the radius R_0. From Table 2 we find that the total luminosity of M 81 with its companions is $L_B(M\ 81) = 3.47 \times 10^{10} L_\odot$. For NGC 2403 with its companions we find $L_B(\mathrm{NGC\ 2403}) = 0.66 \times 10^{10} L_\odot$. Therefore, we obtain a ratio of the total mass within R_0 to the total luminosity in the same volume of

$$M_0/L_B = (38 \pm 7) \cdot M_\odot/L_\odot.$$

Thus the total mass of the two subgroups, M 81+NGC 2403, is 1.2×10^{12} $M_\odot$ via the virial theorem, and 2.0×10^{12} $M_\odot$ via the orbital motions. Their average agrees well with the M_0 estimate. Since the virial and orbital mass estimates trace the mass of the subgroups on a scale of $\leq$200 kpc, we suggest that the total estimated mass, M_0, is concentrated within a compact volume around the two main members of the group, but not spread over the whole 1 Mpc^3 volume. A similar situation takes place in the Local Group, where the total mass within R_0 is also in good agreement with the sum of orbital mass estimates for Milky Way and M 31 subgroups (Karachentsev & Makarov 2001).

The existence of the correlation between the luminosity of spiral galaxies and the amplitude of their rotation (Tully & Fisher 1977) means that the distribution of dark matter (halos) follows closely the distribution of luminous matter. The kinematics of the M 81 subgroup provides us with unique opportunity to test this assumption. The main part ($\sim$90%) of the subgroup luminosity belongs to M 81 and M 82. Their corrected radial velocities are +106 and +360 km s^{-1}, respectively. With regard to the mean velocity of the centroid, $V_c = (164 \pm 21)$ km s^{-1}, the galaxies have peculiar velocities of -58 km s^{-1} (M 81) and +196 km s^{-1} (M 82). To satisfy the law of conservation of motion, the galaxies should have the mass ratio $M_{\mathrm{M\ 81}}/M_{\mathrm{M\ 82}} = 196/58 \sim 3.4$. In fact, this value is very close to the luminosity ratio of these galaxies, $(L_{\mathrm{M\ 81}}/L_{\mathrm{M\ 82}})_B = 2.9$. This would not be the case if the dark virial mass were distributed over the whole volume of the subgroup.

Note, that the total mass-to-total luminosity ratio $(38 \pm 7) M_\odot/L_\odot$, derived by us for the M 81 group, is considerably lower than the value of 174 $M_\odot/L_\odot$ presented by Tully (1987) in his catalogue. As one can see, the high excess of virial mass in Tully's estimate is caused mainly by two reasons: by including the background galaxy NGC 5423 ($D = 5.3$ Mpc, Sharina et al. 1999) into the group, and by neglecting the observed dumb-bell structure of the M 81/NGC 2403 group. This considerably increases both the dispersion of radial velocities and the projected harmonic radius. In the Tully catalog the median virial mass-to-luminosity ratio is 94 $M_\odot/L_\odot$. In this

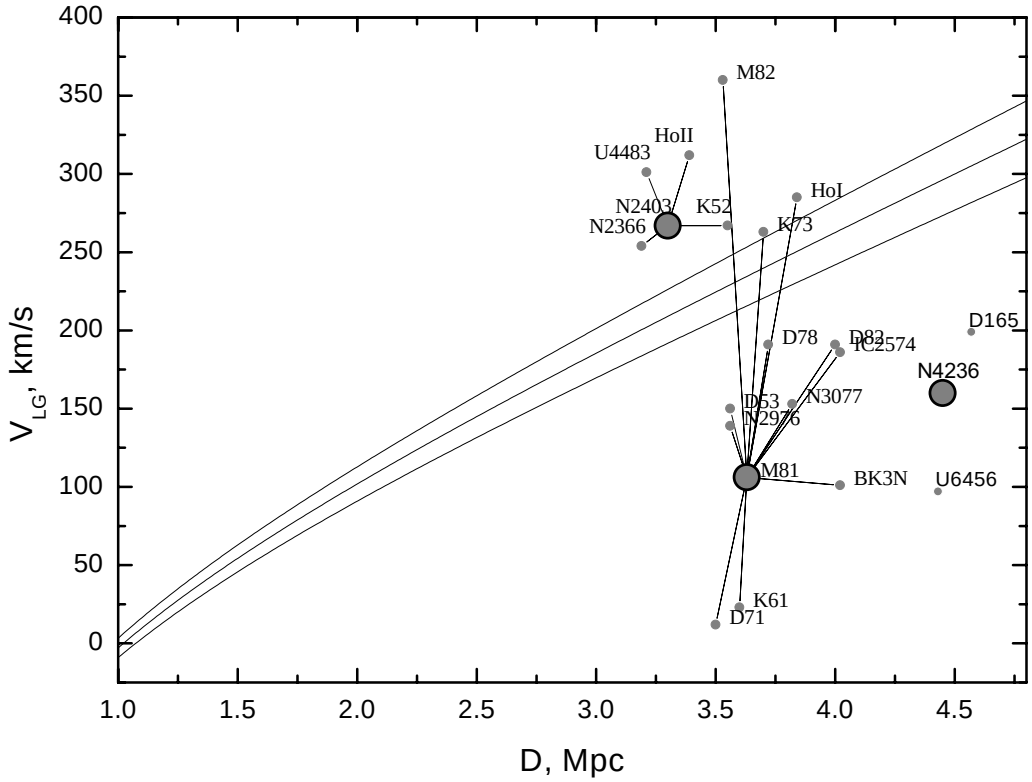

Fig. 9. Distribution of galaxies in the M 81 complex with accurate distance estimates on the Hubble diagram. The three lines correspond to the Hubble relation with $H_0 = 65$, 70, and 75 km s^{-1} Mpc^{-1}, and the Local Group mass 1.5×10^{12} $M_\odot$. The companions of M 81 and NGC 2403 are joined with the principal galaxies by straight lines.

respect the Local Group and M 81 group with their low values: 23 and 38 $M_\odot/L_\odot$ appear to be untypical groups. However, the application of a new, improved algorithm for group selection shows that the groups in the Local Supercluster (of number $N \sim 800$) have the median ratio $M_{\rm vir}/L \sim 30$ $M_\odot/L_\odot$ (Makarov & Karachentsev 2000). Consequently, the dynamical situation in the two best studied nearby groups is not unusual.

6. Concluding remarks

Impressive recent progress in the measurement of accurate distances to many nearby galaxies (measured independently of their velocities) provides the opportunity to study the local peculiar velocity field. Mapping the velocity field of the known nearby groups, like M 81, Centaurus A, Sculptor etc., allows one to determine the total mass of a group via the radius of the zero-velocity surface (Sandage 1986), and to compare such estimates with mass estimates from internal virial motions. As seen from Table 2, our data on accurate distances to galaxies in the M 81 region are still incomplete. Among the 59 objects listed in the table, 5 galaxies have indirect distance estimates based on assumed membership, and 12 galaxies have distances estimated via their brightest stars. Comparison of the distance moduli measured through different methods for the dozen galaxies discussed in Sect. 3 shows that the method of the brightest stars gives moduli with a mean-square error of 0.52 mag, but essentially without a zero-point error, which amounts to -0.01 ± 0.16 mag respect to the TRGB method.

Important cosmological information can be extracted also from the peculiar velocity dispersion of the centers of groups and field galaxies with respect to the Hubble flow. For instance, in the vicinity of the Local Group on the scale of (1–3) Mpc the mean-square non-Hubble velocity of galaxies is only $\sim$25 km s^{-1} (Karachentsev & Makarov 2001), which imposes a strong limitation on the average density of matter, $\Omega_{\rm m}$, in the Local volume (Governato et al. 1997; Klypin et al. 2002).

Figure 9 shows the distribution of the M 81 group galaxies in the Hubble diagram. Here we present only galaxies with well determined distances. The three lines correspond to Hubble constants of $H_0 = 65$, 70, and 75 km s^{-1} Mpc^{-1}. The effect of deceleration due to the Local Group with a total mass of $M_{\rm LG} = 1.5 \times 10^{12}$ $M_\odot$ is taken into account. The companions of M 81 and NGC 2403 are joined with the corresponding principal galaxies by straight lines. As one can see, the M 81 galaxy deviates rather significantly from the Hubble regression lines. However, the M 81 subgroup centroid with

$D_c = 3.70$ Mpc and $V_c = +164$ km s^{-1} has a lower peculiar velocity than M 81 itself. Centroids of the M 81 and NGC 2403 subgroups are situated on opposite sides with respect to the Hubble regression, because they approach each other. As a result, the centroid of the whole M 81/NGC 2403 group has a rather small peculiar velocity, $V_{pec} < 35$ km s^{-1}, when the Hubble parameter H_0 is 60–70 km s^{-1} Mpc^{-1}. The galaxy NGC 4236 and its neighbours DDO 165, UGC 6456 are situated much below the Hubble regression lines. Apparently, being behind the M 81 group, they experience acceleration toward both M 81 and the Local Group.

As was emphasized by Peebles (1989), the knowledge of accurate positions and velocities of all the nearest galaxies enables us to make a choice between competing theories of the origin of small-scale structure of the Universe.

Acknowledgements. Support for this work was provided by NASA through grant GO–08601.01–A from the Space Telescope Science Institute, which is operated by the Association of Universities for Research in Astronomy, Inc., under NASA contract NAS5–26555. D.G. acknowledges financial support for this project received from CONICYT through Fondecyt grant 8000002. This work has also been partially supported by RFBR grant 01–02–16001.

The Digitized Sky Surveys were produced at the Space Telescope Science Institute under U.S. Government grant NAG W-2166. The images of these surveys are based on photographic data obtained using the Oschin Schmidt Telescope on Palomar Mountain and the UK Schmidt Telescope. The plates were processed into the present compressed digital form with the permission of these institutions.

The National Geographic Society – Palomar Observatory Sky Atlas (POSS-I) was made by the California Institute of Technology with grants from the National Geographic Society.

References

Appleton, P. N., Davies, R. D., & Rubin, V. C. 1981, MNRAS, 195, 327
Arp, H. 1982, ApJ, 256, 54
Arp, H. C. 1965, Nature, 148, 363
Bahcall, J. N., & Tremaine, S. 1981, ApJ, 244, 805
Barbieri, C., Bertola, F., & di Tullio, G. 1974, A&A, 35, 463
Börngen, F., & Karachentseva, V. E. 1982, Astron. Nachr., 303, 189
Boyce, P. J., Minchin, R. F., Kilborn, V. A., et al. 2001, ApJ, 560, L127
Caldwell, N., Armandroff, T. E., Da Costa, G. S., & Seitzer, P. 1998, AJ, 115, 535
Da Costa, G. S., & Armandroff, T. E. 1990, AJ, 100, 162
Davidge, T. J., & Jones, J. H. 1989, AJ, 97, 1607
Dolphin, A. E. 2000a, PASP, 112, 1383
Dolphin, A. E. 2000b, PASP, 112, 1397
Dolphin, A. E., Geisler, D., Grebel, E. K., et al. 2002, in preparation
Dolphin, A. E., Makarova, L. N., Karachentsev, I. D., et al. 2001, MNRAS, 324, 249
de Vaucouleurs, G. 1978, ApJ, 224, 710
Efremov, Yu. N., Karachentsev, I. D., & Karachentseva, V. E. 1986, Astron. Zh. Lett., 12, 434
Ferrarese, L., Mould, J. R., Kennicutt, R. C., et al. 2000, ApJ, 529, 745
Fisher, J. R., & Tully, R. B. 1979, AJ, 84, 62
Freedman, W. L., Hughes, S. M., Madore, B. F., et al. 1994, ApJ, 427, 628
Freedman, W. L., & Madore, B. F. 1988, ApJ, 332, L63
Georgiev, Ts.B., Tikhonov, N. A., Karachentsev, I. D., & Bilkina, B. I. 1991, A&AS, 89, 529
Gottesman, S. T., & Veliachev, L. 1975, ApJ, 195, 23
Governato, F., Moore, B., Cen, R., et al. 1997, New Astron., 2, 91
Grebel, E. K., Dolphin, A. E., Geisler, D., et al. 2002, in preparation
Heithausen, A., & Walter, F. 2000, A&A, 361, 500
Hopp, U., & Schulte-Ladbeck, R. E. 1987, A&A, 188, 5
Huchtmeier, W. K., & Skillman, E. D. 1998, A&AS, 127, 269
Karachentseva, V. E. 1968, Comm. Byurakan Obs., 39, 61
Karachentseva, V. E., Karachentsev, I. D., & Börngen, F. 1985, A&AS, 60, 213
Karachentsev, I. D. 1996, A&A, 305, 33
Karachentsev, I. D., & Karachentseva, V. E. 1984, Astrofiz., 21, 641
Karachentsev, I. D., Karachentseva, V. E., & Börngen, F. 1985, MNRAS, 217, 731
Karachentsev, I. D., Karachentseva, V. E., Dolphin, A. E., et al. 2000, A&A, 363, 117
Karachentsev, I. D., & Makarov, D. I. 2001, Astrofiz., 44, 5
Karachentsev, I. D., & Tikhonov, N. A. 1994, A&A, 286, 718
Karachentsev, I. D., Tikhonov, N. A., Georgiev, Ts.B., et al. 1991, A&A, 91, 503
Karachentsev, I. D., Tikhonov, N. A., & Sazonova, L. N. 1994, A&AS, 106, 555
Karachentsev, I. D., Sharina, M. E., Dolphin, A. E., et al. 2001, A&A, 375, 359
Karachentsev, I. D., Sharina, M. E., Grebel, E. K., et al. 1999, A&A, 352, 399
Klypin, A. A., Hoffman, Y., Kravtsov, A. V., & Gottlober, S. 2002 [astro-ph/0107104]
Lee, M. G., Freedman, W. L., & Madore, B. F. 1993, ApJ, 417, 553
Lo, K. Y., & Sargent, W. L. W. 1979, ApJ, 227, 756
Limber, D. N., & Mathews, W. G. 1960, ApJ, 132, 286
Lynden-Bell, D., Faber, S. M., Burstein, D., et al. 1988, ApJ, 326, 19
Lynds, R., Tolstoy, E., O'Neil, E. J., & Hunter, D. A. 1998, AJ, 116, 146
Makarova, L. N. 1999, A&AS, 139, 491
Makarov, D. I., & Karachentsev, I. D. 2000, ASP Conf. Ser., ed. M. J. Valtonen, & C. Flynn, 209, 40
Peebles, P. J. 1989, J. Roy. Astron. Soc. Can., 83, 363
Sakai, S., & Madore, B. F. 1999, ApJ, 526, 599
Sakai, S., & Madore, B. F. 2001, ApJ, 555, 280
Sakai, S., Madore, B. F., & Freedman, W. L. 1996, ApJ, 461, 713
Sandage, A. 1984, AJ, 89, 621
Sandage, A. 1986, ApJ, 307, 1
Sandage, A., & Bedke, J. 1988, Atlas of galaxies useful for measuring the cosmological distance scale, NASA, Washington
Schlegel, D. J., Finkbeiner, D. P., & Davis, M. 1998, ApJ, 500, 525
Sharina, M. E. 1991, Astron. Zh. Lett., 17, 904

Sharina, M. E., Karachentsev, I. D., & Tikhonov, N. A. 1999, Astron. Zh. Lett., 25, 322
Sharina, M. E., Karachentsev, I. D., & Burenkov, A. N. 2002, A&A, accepted
Seitzer, P., Dolphin, A. E., Geisler, D., et al. 2002, in preparation
Seitzer, P., Grebel, E. K., Dolphin, A. E., et al. 1999, BAAS, 195, 8.01
Tammann, G. A., & Sandage, A. 1968, ApJ, 151, 825
Tikhonov, N. A., Bilkina, B. I., Karachentsev, I. D., et al. 1991, A&AS, 89, 1
Tikhonov, N. A., & Karachentsev, I. D. 1993, A&A, 275, 39
Tikhonov, N. A., Karachentsev, I. D., Bilkina, B. I., et al. 1992, A&A, 1, 269
Tully, R. B., & Fisher, J. R. 1977, A&A, 54, 661
Tully, R. B. 1987, ApJ, 321, 280
van Driel, W., Kraan-Korteweg, R. C., Binggeli, B., & Huchtmeier, W. K. 1998, A&AS, 127, 397
Yun, M. S., Ho, P. T. P., & Lo, K. Y. 1994, Nature, 372, 530